Calorimetric Dissection of Colicin DNase−Immunity Protein Complex Specificity†

Anthony H. Keeble,‡,§ Nadine Kirkpatrick,‡ Seishi Shimizu,|| and Colin Kleanthous*,‡

Department of Biology (Area 10), Post Office Box 373, University of York, Heslington, York YO10 5YW, United Kingdom, and York Structural Biology Laboratory, Department of Chemistry, University of York, Heslington, York YO10 5YW, United Kingdom

Received November 21, 2005; Revised Manuscript Received January 17, 2006

ABSTRACT: We explore the thermodynamic strategies used to achieve specific, high-affinity binding within a family of conserved protein−protein complexes. Protein−protein interactions are often stabilized by a conserved interfacial hotspot that serves as the anchor for the complex, with neighboring variable residues providing specificity. A key question for such complexes is the thermodynamic basis for specificity given the dominance of the hotspot. We address this question using, as our model, colicin endonuclease (DNase)−immunity (Im) protein complexes. In this system, cognate and noncognate complexes alike share the same mechanism of association and binding hotspot, but cognate complexes ($K_d \sim 10^{-14}$ M) are orders of magnitude more stable than noncognate complexes (10^6-10^{10}-fold discrimination), largely because of a much slower rate of dissociation. Using isothermal titration calorimetry (ITC), we investigated the changes in enthalpy (ΔH), entropy ($-T\Delta S$), and heat capacity (ΔC_p) accompanying binding of each Im protein (Im2, Im7, Im8, and Im9) to the DNase domains of colicins E2, E7, E8, and E9, in the context of both cognate and noncognate complexes. The data show that specific binding to the E2, E7, and E8 DNases is enthalpically driven but entropically driven for the E9 DNase. Analysis of ΔC_p, a measure of the change in structural fluctuation upon complexation, indicates that E2, E7, and E8 DNase specificity is coupled to structural changes within cognate complexes that are consistent with a reduction in the conformational dynamics of these complexes. In contrast, E9 DNase specificity appears coupled to the exclusion of water molecules, consistent with the nonpolar nature of the interface of this complex. The work highlights that although protein−protein interactions may be centered on conserved structural epitopes the thermodynamic mechanism underpinning binding specificity can vary considerably.

Understanding the thermodynamic basis for specificity in protein−protein interactions is key to deciphering the networks of interprotein complexes that underpin cellular function. A thorough understanding of such interactions and in particular the basis for specific recognition requires knowledge of the structure as well as kinetics and thermodynamics (*1*−*4*). In contrast to the structural and kinetic basis for protein−protein recognition, which has been the focus of numerous previous studies, our understanding of the underlying thermodynamics of protein−protein complexes is still rudimentary. In the present work, we focus on a large (16 member) family of conserved protein−protein complexes in which binding occurs across the whole spectrum of biologically relevant K_d values (milli−femtomolar) to gain insight into the thermodynamic basis of protein recognition specificity.

The E colicin DNases are a group of bacterial toxins (E2, E7, E8, and E9)[1] that kill target microbial cells through random degradation of chromosomal DNA (*5*). To avoid suicide, producing strains co-synthesize an immunity protein (Im2, Im7, Im8, and Im9) specific for each colicin that neutralizes the catalytic activity of the toxin (*6*). Colicin DNases and their Im proteins form two families of highly conserved (65 and 50% sequence identity, respectively) and divergently evolved proteins (*6*). Im proteins do not bind within the active site of the DNase domains, as is the case for most nuclease−inhibitor complexes; instead, they bind at an exosite, illustrated in Figure 1 for the E9 DNase−Im9 complex. The active site is adjacent to the Im-binding site and is made up of a metal ion embedded within a so-called HNH motif (*7*, *8*). Inhibition results from steric and electrostatic clashes between the negatively charged Im protein (pI ∼ 4.5) and the phosphates of substrate DNA. Exosite binding explains how novel immunity-protein-binding specificities have arisen because chemically diverse interfaces can evolve without compromising the catalytic activity of the enzyme (*9*). In line with this, the Im protein exosite (IPE) on a colicin DNases (residues 72−98) is hypervariable in sequence in an otherwise highly conserved family of proteins (Figure 1b).

† This work was supported by a grant from the Biotechnology and Biological Sciences Research Council of the U.K. (to C.K.) and an award from the Nuffield Foundation (to S.S.).

* To whom correspondence should be addressed. Telephone: +44-(0)-1904-328820. Fax: +44-(0)-1904-328825. E-mail: ck11@york.ac.uk.

‡ Department of Biology.

§ Present address: MRC Laboratory of Molecular Biology, Hills Road, Cambridge, CB2 2QH, U.K.

|| Department of Chemistry.

[1] Abbreviations: E2, E7, E8, and E9 DNase, endonuclease domain of colicins E2, E7, E8, and E9, respectively; Im2, Im7, Im8, and Im9, immunity proteins specific for the respective colicin DNase; Mops, 3-(*N*-morpholino)propanesulfonic acid; PIPES, piperazine-1,4-bis(2-ethanesulfonic acid); $\langle H \rangle^2 - \langle H^2 \rangle$, the enthalpy fluctuations of a system; ITC, isothermal titration calorimetry.

10.1021/bi052373o CCC: $33.50
Published on Web 02/18/2006

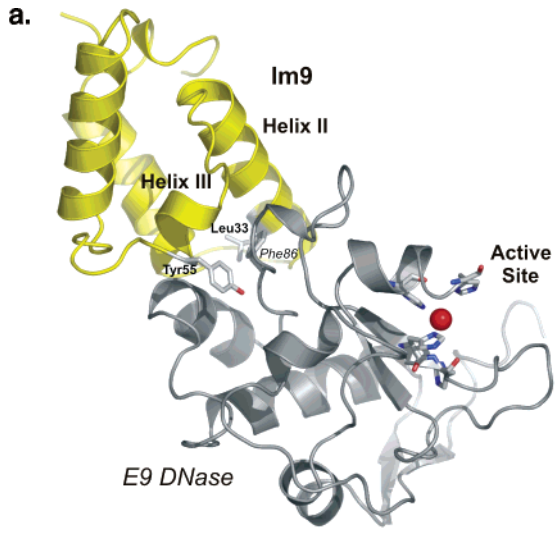

b. Im protein binding region on colicin DNases

```
    54  70                                  99
E2  R...QFKGSNKTNIQKGKAPFARKKDQVGGRERF
E7  R...QFSRNNNDRMKVGKAPKTRTQDVSGKRTSF
E8  R...QFNPGNKKRLSQGLAPRARNKDTVGGRRSF
E9  R...NLNPSNKSSVSKGYSPFTPKNQQVGGRKVY
```

c. Colicin DNase binding region on Im proteins

```
    20                                  62
Im2 VKKICRAEGATEEDDNKLVREFERLTEHPDGSDLIYYPRDDRED
Im7 LKEIEKENVATDDVLDVLLEHFVKITEHPDGTDLIYYPSDNRDD
Im8 IEDIINCE-GDEKKQDDNLEHFISVTEHPSGSDLIYYPEGNNDG
Im9 VTTICNADTSSEEELVKLVTHFEEMTEHPSGSDLIYYPKEGDDD
```

FIGURE 1: (a) Crystal structure of the E9 DNase−Im9 complex showing the location of the active site relative to the Im protein. The E9 DNase is colored gray, and Im9 is in yellow. Also shown are the side chains of the active-site histidines that bind the single metal ion (red sphere) and key interface residues (Phe86 from the IPE on the DNase and Leu33 and Tyr55 from helices II and III of Im9, respectively) (PDB code 1bxi) (*7*). (b) Sequence alignment of the IPE on the four DNases. (c) Sequence alignment of the DNase binding site on the four Im proteins. Assignment of buried residues for the E7 DNase−Im7 and E9 DNase−Im9 complexes is based on the published crystal structures, with buried residues for the other two complexes based on these (*21*, *22*). Buried residues are in bold and colored according to residue type and how they are buried: black signifies a buried residue that is not part of the protein−protein interface; blue signifies nonpolar residues; green signifies polar residues; red signifies charged residues. Underlined residues for the E7 DNase−Im7 and E9 DNase−Im9 complexes indicate that the backbone rather than the side chain is mediating the interaction. For the E9 DNase, two lysines are colored blue because only the hydrophobic portions of the residues become buried on Im9 binding (*7*, *21*).

Colicin DNase−Im protein interactions accommodate two strikingly different capabilities: promiscuous binding, because all 16 possible DNase−Im protein combinations can form complexes (K_d values ranging from 10^{-4} to 10^{-15} M), yet highly specific complex formation, with cognate complexes binding 10^6−10^{10}-fold tighter than noncognate complexes (*10*−*12*). Mutagenesis of residues in the two helices of the Im protein that comprise the DNase-binding site has led to the proposal that specificity is governed by a "dual recognition" mechanism. Conserved elements (helix III) of the Im protein anchor the binding of both cognate and noncognate complexes, making sequence-independent interactions, largely with the DNase backbone. Helix II harbors specificity residues that contribute to the higher affinities of cognate complexes, which stabilize cognate complexes and likely destabilize noncognate complexes (*6*, *12*−*16*). Dual recognition in colicin DNase−Im protein complexes has many similarities to other conserved protein−protein interactions, notably SH2−phosphopeptide and TCR−peptide−MHC complexes (*12*).

On the basis of detailed kinetic analysis of DNase−Im protein complexes, a model has been proposed that provides a framework for understanding the basis for dual recognition (*16*). Cognate and noncognate complexes bind with similar association rate constants to form an initial, low-affinity (10^{-6}−10^{-8} M), encounter complex, which is stabilized by conserved sequence elements of the interface. This then undergoes conformational rearrangements that take the form of rigid-body rotations rather than classical "induced-fit" changes. This allows for a kinetic read-out of specificity to occur as variable sequence elements on the immunity protein "search" for their partners on the DNase. In a cognate context, these contacts "lock" the complex into a single high-affinity conformation. In a noncognate complex, this locking step does not occur and therefore conformational (rotational) dynamics remain. Thus, the distinction between cognate and noncognate binding arises from the dissociation kinetics with cognate complexes dissociating 10^6−10^7-fold slower than noncognate, a feature conserved for all colicin DNases (*12*).

Thus far, all previous papers on the basis for dual recognition in colicin DNase−Im protein complexes have focused on using kinetic analysis in conjunction with protein engineering (*7*, *10*−*16*) and structural studies (*17*−*22*). Consequently, the thermodynamic basis for binding and specificity remains poorly understood. In the present work, we have used ITC to measure directly the changes in heat accompanying binding for all 16 possible colicin DNase−Im protein complexes. This shows that the four DNases use strikingly different thermodynamic strategies to achieve specific binding to Im proteins, despite using conserved kinetic strategies. We go on to discuss the thermodynamic basis for specificity in DNase−Im protein complexes in the context of other protein−protein interactions and propose physical models for specificity in these complexes.

MATERIALS AND METHODS

Protein Purification and Quantification. All colicin DNase domains and Im proteins were purified, and their concentrations were determined using previously described methods (*5*, *10*, *11*).

Isothermal Titration Calorimetry (ITC). Experiments were carried out using a VP-ITC (Microcal) calorimeter according to the instructions of the manufacturer. Briefly, lyophilised protein samples were extensively dialyzed overnight at 4 °C into the assay buffer [50 mM 3-(*N*-morpholino)propanesulfonic acid (Mops) at pH 7.0 containing 200 mM NaCl], with either the DNase prebound with Zn^{2+} or in its absence, and centrifuged in a benchtop microfuge at 13 000 rpm for 5−10 min to remove aggregates. The assay buffer was filtered (0.22 μM pore size) before protein samples were diluted to the working concentration, which were then degassed immediately prior to use. Experiments were run either at 298 K (for all 16 DNase−Im protein complexes)

Table 1: Thermodynamic Parameters for Cognate DNase−Immunity Protein Complexes[a]

complex	*n*	ΔG (kcal/mol)[b]	ΔH_{obs} (kcal/mol)[c]	$-T\Delta S$ (kcal/mol)[d]	T_m (°C)[e]
E2 Im2 ($-Zn^{2+}$)	0.94	−19.64 (±0.07)	−38.64 (±0.17)	19.00	37.3
E2 Im2 ($+Zn^{2+}$)	1.00	−19.64 (±0.07)	−33.09 (±0.03)	13.45	61.2
E7 Im7 ($-Zn^{2+}$)	0.93	−19.8	−56.73 (±0.2)	36.9	26.3
E7 Im7 ($+Zn^{2+}$)	1.11	−19.8	−30.34 (±0.75)	10.5	59.9
E8 Im8 ($-Zn^{2+}$)	1.05	−19.8	−25.84 (±0.19)	6.04	45.5
E8 Im8 ($+Zn^{2+}$)	1.05	−19.8	−24.23 (±0.23)	4.43	63.7
E9 Im9 ($-Zn^{2+}$)	0.91	−18.57 (±0.09)	−19.0 (±0.3)	0.42	36.6
E9 Im9 ($+Zn^{2+}$)	0.98	−18.57 (±0.09)	−10.51 (±0.44)	−8.07	63.0

[a] ITC experiments were carried out in the presence ($+Zn^{2+}$) or absence ($-Zn^{2+}$) of a bound metal ion within the active site of the DNase (see the text for details). [b] ΔG values are from Li et al. (*12*) and shown previously to be independent of bound Zn^{2+} (*24*). Values for E2 DNase−Im2 and E9 DNase−Im9 were experimentally determined using a combination of stopped-flow kinetics (k_{on}) and radioactive subunit exchange kinetics (k_{off}), where $K_d = k_{off}/k_{on}$ and ΔG is calculated using eq 1 (*10*, *12*). In the case of the E7 DNase−Im7 and E8 DNase−Im8 complexes, ΔG was based on a measured k_{on} but a predicted a k_{off} predicted to be the same as for the other DNase−Im complexes (see the text for details). Preliminary k_{off} experiments focusing on the E7 DNase−Im7 complex indicate that k_{off} is similar to that for E2 DNase−Im2 and E9 DNase−Im9 (data not shown). [c] ΔH was determined directly in each case from the binding isotherm. [d] $-T\Delta S$ was calculated using eq 1, on the basis of the derived values of ΔG and ΔH. [e] Transition-point temperature for the thermal denaturation of the DNases determined by differential scanning calorimetry (*25*, *26*). *n*, observed stoichiometry. The data are the averages of two independent observations with the errors shown in parentheses. Conditions: 50 mM Mops at pH 7.0 and 200 mM NaCl at 25 °C.

or in the range of 288−303 K for those complexes in which the change in heat capacity at constant pressure (ΔC_p) was being determined. The concentrations of proteins used in each experiment and the size and number of injections used varied depending upon the observed heats produced during the experiment. After the subtraction of the heats of dilution, the resulting binding isotherm was fitted to a 1:1 binding model using the software of the manufacturer to directly obtain the ΔH and the affinity constant, K_a, and from this the equilibrium K_d.

RESULTS

Cognate Complexes Use Different Thermodynamic Strategies To Achieve High-Affinity Binding. While kinetic analysis of DNase−Im protein binding has enabled the change in free energy (ΔG) upon binding to be determined, it does not allow for the enthalpic (ΔH) or entropic ($-T\Delta S$) contributions to binding to be evaluated, as defined by eq 1

$$\Delta G = RT \ln K_d = \Delta H - T\Delta S \quad (1)$$

where R is the molar gas constant and T is the temperature. The thermodynamics of binding are coupled to changes in the protein structure and hydration, and therefore, their quantification can provide important mechanistic insights. This is particularly important given the dynamic nature of proteins in solution (*23*). Understanding the underlying thermodynamics also provides important information on the different thermodynamic strategies that may be adopted, particularly for conserved protein complexes that may have the same binding affinity (K_d).

Cognate colicin DNase−Im protein complexes show similar high-affinity binding; the K_d for these complexes (where $K_d = k_{off}/k_{on}$) is $\sim 10^{-14}$−10^{-15} M in 200 mM salt. Rapid-reaction kinetics has shown that all four cognate complexes (E2 DNase−Im2, E7 DNase−Im7, E8 DNase−Im8, and E9 DNase−Im9) bind with a very rapid association rate constant ($k_{on} \sim 10^8$ M^{-1} s^{-1}) (*10*, *12*). Radioactive subunit exchange kinetics has shown that for the E2 DNase−Im2 and E9 DNase−Im9 complexes this is complemented by a very slow dissociation rate constant ($k_{off} \sim 10^{-6}$ s^{-1}) (*10*, *12*). Although k_{off} measurements have not been completed for the E7 DNase−Im7 and E8 DNase−Im8 complexes, we suggest that they likely take similar values for a number of reasons. First, the formation of all four cognate complexes achieves the same role in vivo, namely, the efficient inhibition of the cytotoxic activity of the DNase domain by the Im protein. Second, that the four pairs of proteins show high structural and overall sequence conservation. Third, that despite the protein−protein interface between the DNase and Im protein being sequence-divergent the E2 DNase−Im2 and E9 DNase−Im9 complexes have very similar k_{off} values. Fourth, that all four complexes can only be separated by high concentrations of denaturants. Finally, that similarly very slow dissociation rate constants are a conserved feature of many other nuclease−inhibitor complexes such as barnase−barstar and ribonuclease inhibitor−RNase A (*8*). Thus, the ΔG values cited in Table 1 for the E7 DNase−Im7 and E8 DNase−Im8 complexes are based on experimentally determined k_{on} values and predicted k_{off} values with the larger errors reflecting this.

To understand the molecular basis for such high affinities, we used ITC to measure the changes in heat accompanying the binding of all four cognate complexes (Figure 2 and Table 1). Binding in ITC experiments shows a "steplike" transition characteristic of stoichiometric binding in which the concentration of the reactants is >500-fold higher than the K_d, thus precluding accurate data fitting and hence the measurement of K_d (*23*). Binding of Zn^{2+} within the active site of the DNase does not affect the kinetics or K_d for Im protein binding (*24*) but does increase the thermal stability of each DNase by 15−30 °C, resulting in the Zn^{2+}-bound DNases all having similar melting temperatures (~60 °C) (*25*, *26*). Hence, Im protein binding was carried out on both apo- and Zn^{2+}-bound DNases to address to what extent the changes in enthalpy (ΔH) and entropy (shown as $-T\Delta S$) accompanying binding reflect differences in the thermal stabilities of the DNases (Table 1) and therefore the global effects of binding. In all cases, binding was enthalpically favorable, with binding to the apo-DNase always more enthalpically favorable (and less entropically favorable) than to the Zn^{2+}-bound form (Table 1). The difference between the apo- and Zn^{2+}-bound states of the DNase is largest for the most unstable, metal-free DNase (E7, $T_m \sim 26$ °C) and smallest for the most stable metal-free DNase (E8, T_m

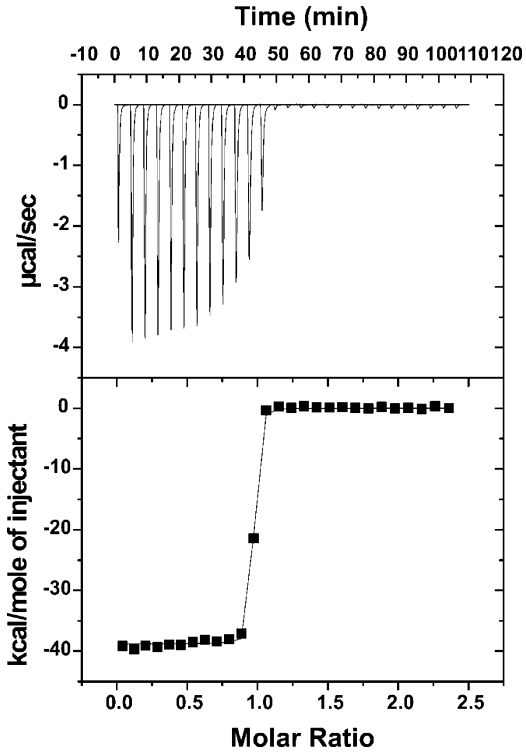

FIGURE 2: ITC binding isotherm for the cognate E2 DNase ($-Zn^{2+}$) binding Im2 at 298 K. Data were analyzed using a 1:1 binding model (see the Materials and Methods for details). Derived values for ΔG [determined kinetically (*12*)] and other thermodynamic parameters are listed in Table 1.

$\sim$ 45 °C), suggesting that binding-induced stabilization/folding occurs upon binding of Im proteins to metal-free DNases. Certainly, the very negative ΔH observed for the metal-free E7 DNase binding Im7 is characteristic of binding-induced folding (*27*). In the case of the other metal-free DNase domains, the temperature at which the experiment was carried out (25 °C) was well below (>10 °C) their measured T_m values, suggesting that Im protein binding in these cases stabilizes the protein rather than inducing global folding per se. To eliminate binding-induced stabilization/folding contributions to the observed thermodynamic parameters, all of our experiments were subsequently focused on using Zn^{2+}-bound DNases. All Im proteins have similarly high thermal stabilities ($T_m \sim 55$ °C). Importantly, inclusion of Zn^{2+} ions in all of our ITC experiments while having a global effect on the observed ΔH has no direct impact on the formation of colicin DNase−Im protein complexes. The metal ion forms no part of the interface (Figure 1), and crystal structures of apo- and metal-ion-bound DNase−Im protein complexes show identical protein−protein interfaces (*21*).

Table 1 (shown graphically in Figure 4) shows that significant differences in the thermodynamics of Im protein binding at 25 °C are observed for the Zn^{2+}-bound DNases. The favorable enthalpic contribution decreases in the order E2 (most favorable) > E7 >E8 > E9 (least favorable) with a corresponding pattern seen also for the binding entropies ($-T\Delta S$), with binding to the E2, E7, and E8 DNases becoming less entropically unfavorable and binding to the E9 DNase being entropically favored. Hence, while cognate Im protein binding to the E2, E7, and E8 DNases is enthalpically driven, it is both enthapically and entropically driven for the E9 DNase. The data for the E9 DNase−Im9 complex agree with previous values determined by van't Hoff analysis carried out under the same conditions as used in the present work (*10*). Thus, despite the kinetics of binding being conserved, the thermodynamics are variable. Such differential use of distinct thermodynamic strategies by related complexes to achieve similar binding affinities has previously been dubbed "thermodynamic homeostasis" (*28*).

Protonation/Deprotonation Events Are Not Coupled to DNase−Im Protein Binding. Observed enthalpy changes in ITC experiments can be influenced by protonation/deprotonation events. These can be coupled to binding such that the experimentally observed enthalpy change (ΔH_{obs}) is a combination of the true enthalpy change upon binding (ΔH_{bind}) and the enthalpy change of n protonation/deprotonation events ($\Delta H_{ionization}$) as shown in eq 2 (*29*)

$$\Delta H_{obs} = \Delta H_{bind} - n\Delta H_{ionization} \quad (2)$$

Under the conditions used in our experiments (pH 7.0), the only side chain with a pK_a that is likely to be perturbed upon binding and therefore produce a change in the protonation state is histidine. In the case of colicin DNases, histidine residues are only found within the active site (Figure 1), which are not contacted by the Im protein. Few histidines are found in Im proteins, and the few that are present are not surface-exposed and their environment does not change upon binding to the DNase (*7*, *19*). Consistent with this, the kinetics of colicin DNase−Im protein interactions are essentially pH-independent within the pH 5−9 range (*10*). Preliminary experiments carried out in buffers with different enthalpies of ionization showed similar observed enthalpy changes to those presented. For example, in the case of E9 DNase−Im9 binding, ΔH values of −11.4 (±0.1) and −11.3 (±0.1) kcal mol^{-1} were obtained for experiments repeated in cacodylate [$\Delta H_{ionization} = -0.47$ (±0.01) kcal mol^{-1}] and piperazine-1,4-bis(2-ethanesulfonic acid) (PIPES) [$\Delta H_{ionization} = 2.74$ (±0.01) kcal mol^{-1}], which compare well with the value obtained in Table 1 that was measured in Mops [$\Delta H_{ionization} = 5.22$ (±0.01) kcal mol^{-1}] (*31*). We conclude that protonation/deprotonation is not coupled to binding under the conditions of the present ITC experiments.

Analysis of Noncognate DNase−Im Protein Complexes Demonstrates That the Thermodynamic Basis for Specificity Varies between DNases. We next investigated the binding of noncognate complexes by ITC to address the thermodynamic basis for both the high specificity in DNase−Im protein interactions and the promiscuous cross-reactivity of noncognate complexes. In most cases, the K_d values determined by ITC were within 2−4-fold of those previously determined by rapid-reaction kinetics (Table 2). The noncognate complexes of E7 DNase−Im8 and E8 DNase−Im7 binding were too tight to measure by ITC, producing "steplike" binding isotherms that are consistent with their kinetically derived K_d values (10^{-9}−10^{-10} M) (*12*). Of the 10 noncognate K_d values measured by ITC, only two deviated significantly from kinetically derived values. These were for the E9 DNase−Im2 and E7 DNase−Im2 complexes (Figure 3), which are ∼15- and ∼70-fold weaker than the previously determined values. We have shown recently for the E9 DNase−Im2 complex that this overestimate of the kinetically

Table 2: Thermodynamic Parameters for Noncognate DNase−Immunity Protein Binding

complex	K_d (M) (kinetic)[a]	K_d (M) (ITC)[b]	n	ΔG (kcal/mol)[c]	ΔH_{obs} (kcal/mol)[d]	$-T\Delta S$ (kcal/mol)[e]
E2 Im7 ($+Zn^{2+}$)	$1.4\ (\pm0.0) \times 10^{-8}$	$2.44\ (\pm0.45) \times 10^{-8}$	1.04	−10.38 (±0.12)	−10.47 (±0.2)	0.09
E2 Im8 ($+Zn^{2+}$)	$3.4\ (\pm0.4) \times 10^{-8}$	$1.46\ (\pm0.33) \times 10^{-7}$	1.08	−9.32 (±0.15)	−2.45 (±0.11)	−6.89
E2 Im9 ($+Zn^{2+}$)	$1.2\ (\pm0.1) \times 10^{-8}$	$3.14\ (\pm0.7) \times 10^{-8}$	0.96	−10.23 (±0.15)	−0.498 (±0.05)	−9.732
E7 Im2 ($+Zn^{2+}$)	$3.6\ (\pm0.2) \times 10^{-10}$	$2.47\ (\pm0.35) \times 10^{-8}$	0.97	−9.01 (±0.09)	−17.81 (±0.4)	8.8
E7 Im8 ($+Zn^{2+}$)	$3.7\ (\pm0.4) \times 10^{-10}$	$<10^{-9}$	1.07	−12.88 (±0.04)	−5.80 (±0.15)	−7.08
E7 Im9 ($+Zn^{2+}$)	$3.8\ (\pm0.1) \times 10^{-8}$	$1.25\ (\pm0.28) \times 10^{-7}$	1.08	−9.41 (±0.15)	−8.47 (±0.07)	−0.94
E8 Im2 ($+Zn^{2+}$)	$1.8\ (\pm0.1) \times 10^{-8}$	$8.5\ (\pm1.1) \times 10^{-8}$	1.02	−9.64 (±0.08)	−12.56 (±0.04)	2.92
E8 Im7 ($+Zn^{2+}$)	$1.0\ (\pm0.1) \times 10^{-9}$	$<10^{-9}$	0.98	−12.27 (±0.06)	−10.81 (±0.2)	−1.46
E8 Im9 ($+Zn^{2+}$)	$6.4\ (\pm0.2) \times 10^{-8}$	$1.82\ (\pm0.4) \times 10^{-7}$	1.07	−9.19 (±0.02)	−4.56 (±0.31)	−4.63
E9 Im2 ($+Zn^{2+}$)	$1.0\ (\pm0.0) \times 10^{-8}$	$1.54\ (\pm0.4) \times 10^{-7}$	1.06	−9.29 (±0.01)	−7.75 (±0.005)	−1.54
E9 Im7 ($+Zn^{2+}$)	$\sim10^{-4}$	$\sim10^{-4}$	1.00	~ -5.45	~ -1	−4.45
E9 Im8 ($+Zn^{2+}$)	$0.5\ (\pm0.2) \times 10^{-6}$	$1.35\ (\pm0.17) \times 10^{-6}$	1.0	−8.00 (±0.08)	−2.72 (±0.2)	−5.28

[a] Kinetically derived K_d values determined from the ratio of k_{off} and k_{on} have previously been determined by stopped-flow experiments (*12*, *16*). [b] K_d determined from the ITC experiments in the present work (see the Materials and Methods for details). [c] ΔG calculated using eq 1 (see the text for details) and the K_d determined from the present ITC experiments. [d] ΔH was determined directly from the binding isotherm. [e] $-T\Delta S$ was calculated using eq 1, on the basis of the derived values of ΔG and ΔH. In all cases, data shown are the averages of two independent observations, with the errors shown in parentheses.

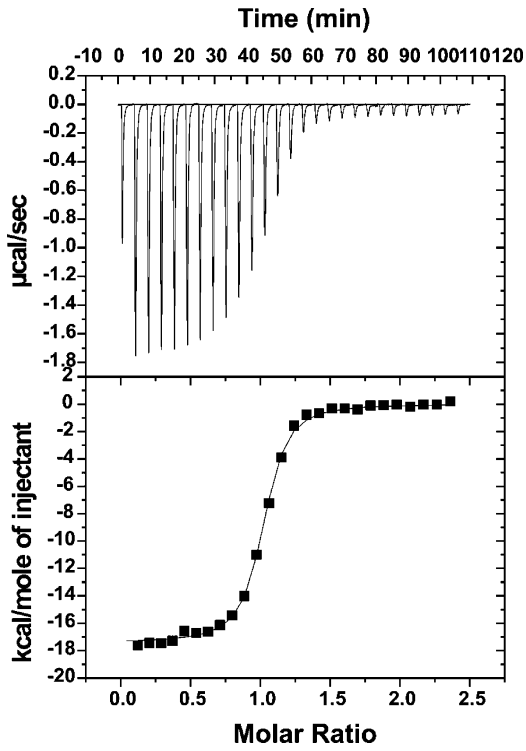

FIGURE 3: ITC binding isotherm for the noncognate complex of E7 DNase ($+Zn^{2+}$) and Im2 at 298 K. Data were analyzed using a 1:1 binding model (see the Materials and Methods for details). Derived values are listed in Table 2.

derived binding affinity is a consequence of the rate-determining step for dissociation being misassigned in stopped-flow experiments (*16*), and the same is likely to be true for the E7 DNase−Im2. In all cases tested (including for the E7 DNase), the presence of bound Zn^{2+} had little effect on the observed K_d values (data not shown), consistent with our previous observations (*24*).

The changes in enthalpy (ΔH) and entropy (shown as $-T\Delta S$) for all 12 noncognate complexes are listed in Table 2 and compared in bar-chart form in Figure 4 with the 4 cognate complexes. The data in Figure 4 show that noncognate complexes are generally less enthalpically favorable than cognate complexes. Hence, specificity is enthalpy-driven for all four cognate colicin DNases complexes, which is suggestive of more favorable interactions relative to their noncognate counterparts. Previous alanine-scanning mutagenesis experiments have shown that cognate complexes indeed use a greater number of residues to stabilize binding than do noncognate complexes (*12*, *14*, *15*). In this context, binding of the cognate complexes for E2, E7, and E8 DNases is entropically very unfavorable despite these binding with much higher affinity than their noncognate complexes, where binding in most cases is entropically favorable. This contrasts the situation with the E9 DNase, where the cognate complex is more entropically favorable than noncognate complexes. It is clear then that two different thermodynamic strategies underpin these systems, one that is shared by the E2, E7, and E8 DNases and one used by the E9 DNase alone.

Variability in the Thermodynamics of Noncognate DNase−Im Protein Binding Has More Than One Source. Noncognate complexes access a broader range of ΔH values than ΔG values, although they are always favorable (at 298 K) (Table 2). Such observations are often referred to as "enthalpy−entropy compensation" (changes in $-T\Delta S$ compensate for those in ΔH, resulting in only small changes in ΔG). However, two underlying trends exist, suggesting that part of the variation may be due to differences in the sequences of the proteins. First, it is noticeable that, for noncognate complexes, binding is most enthalpically favorable for Im2 followed by Im7, with Im8 and Im9 being similar. This pattern mirrors that of the cognate complexes, where the binding enthalpy steadily becomes less favorable in the order Im2 > Im7 > Im8 > Im9. Second, the noncognate complexes become less entropically favorable in the order Im9 > Im8 > Im7 > Im2. This also mirrors the pattern in cognate complexes, to the extent that the entropic contribution of both cognate and noncognate Im protein binding to the E9 DNase follows the above order. "Enthalpy−entropy compensation" is believed to be a consequence of protein−ligand interactions being mediated by multiple weak interactions that also involve water molecules (*29*−*32*), with the variability in observed thermodynamics between complexes linked to the use of different interactions. Indeed, comparative alanine-scanning mutagenesis studies of noncognate complexes (for the E2 DNase−Im9 and E9 DNase−Im2 complexes) show that significant variability in the residues used to stabilize binding exists even between noncognate complexes (*12*).

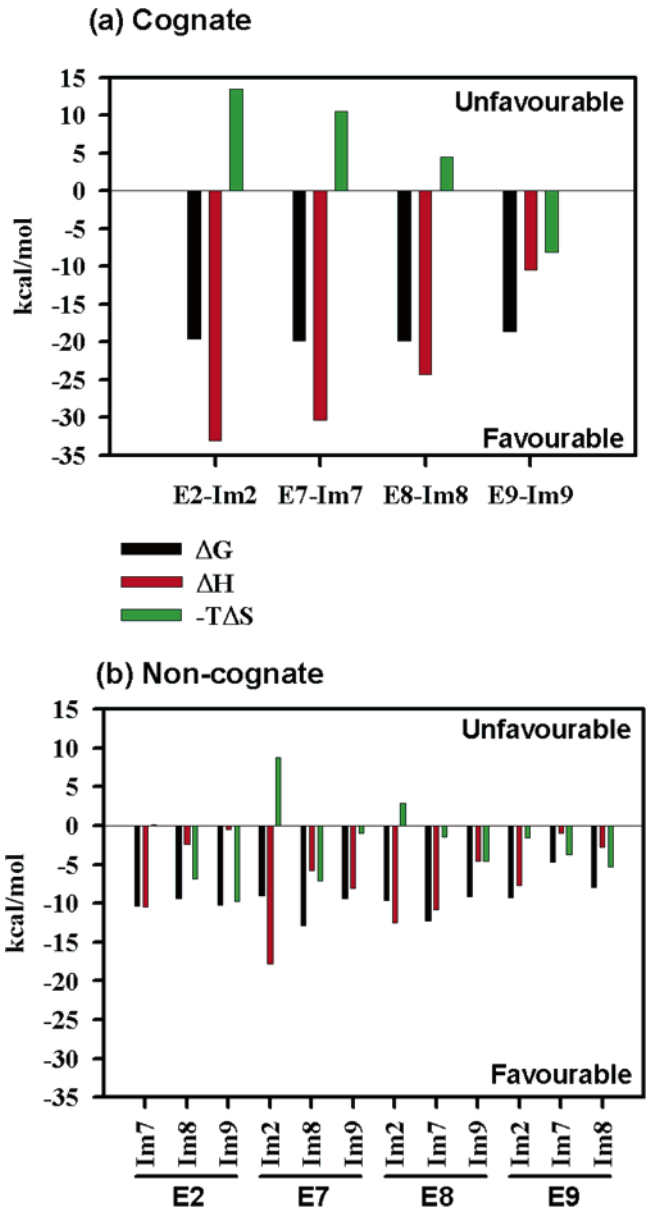

FIGURE 4: Graphical representation of the relative values of ΔG (black), ΔH (red), and $-T\Delta S$ (green) for (a) cognate complexes and (b) noncognate DNase−Im protein complexes. See the text for details.

Heat Capacity Changes Compared for Cognate and Noncognate Complexes. Structural changes accompanying binding, present in the protein or surface coordinated water molecules, are intimately linked to the thermodynamics of binding through the change in heat capacity at constant pressure (ΔC_p) (*23*, *32*). To further investigate the links between structure and thermodynamics for the DNase−Im protein complexes, we determined the ΔC_p for the four cognate complexes by measuring ΔH across a range of temperatures. Applying the standard assumption that ΔC_p is temperature-independent (which holds true over narrow ranges of temperatures such as those used here), then ΔC_p is calculated using eq 3 (*23*, *32*)

$$\Delta C_p = d\Delta H/dT \quad (3)$$

Representative data are shown for the E2 DNase−Im2 complex in Figure 5, and the results for the four cognate

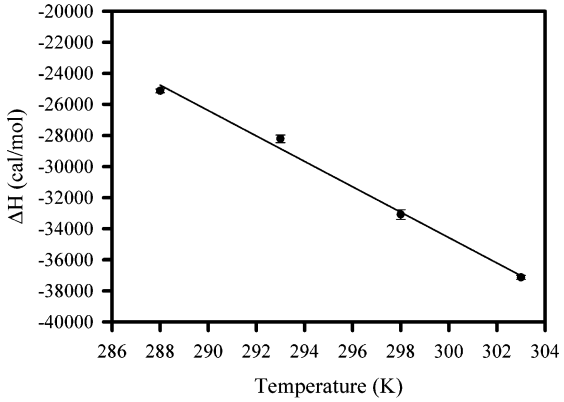

FIGURE 5: ΔC_p for E2 DNase ($+Zn^{2+}$) binding Im2. The observed ΔH was determined at a range of temperatures between 288 and 303 K and plotted against each other, with the ΔC_p (-818 cal mol^{-1} K^{-1}) determined from the slope of a line of best fit to the data. Each of the data points is the average of two independent measurements. See Table 3 for further details.

complexes shown in Table 3. The values for ΔC_p range from -454 to -818 cal mol^{-1} K^{-1}. In comparison, typical values of ΔC_p for protein−protein interactions (in which no large conformational changes occur) are of the order of -100 to -200 cal mol^{-1} K^{-1} (*27*).

Strongly negative ΔC_p values indicate that there is a large burial of hydrophobic surface, either at the protein−protein interface or as the result of coupled binding and folding (*27*). If the latter were occurring, then the observed ΔC_p would be the sum of the ΔC_p of binding and the ΔC_p for the coupled folding (*27*). This would also result in curved ΔH versus temperature plots, which is not the case here. In the present work, ΔC_p values were determined at temperatures where both Im proteins and Zn^{2+}-bound DNases are stable. Furthermore, crystallography and NMR show that both Zn^{2+}-bound DNases and Im proteins have essentially the same fold in the absence of the partner protein (*18*, *20*, *33*). As a result, coupled binding and folding is unlikely to occur. This is underlined by the observation that the ΔC_p for Im protein binding to the apo-E7 DNase, which has a $T_m \sim 26$ °C, is >2000 cal mol^{-1} K^{-1} (data not shown), which strikingly illustrates what is observed when folding is coupled to binding in this system.

The significant differences that we observe in ΔC_p values for the four cognate complexes (in the presence of metal ion) suggest that an explanation other than simple "enthalpy−entropy compensation" underpins the observed differences in the enthalpic and entropic contributions to binding, and these are addressed in the Discussion.

ΔC_p values were also measured for representative noncognate complexes of each DNase (Table 3). For E2, E7, and E8 DNases, ΔC_p for the cognate complex is significantly more negative than for noncognate complexes, while for the E9 DNase, the cognate and noncognate complexes have similar ΔC_p values (slightly more negative for the noncognate). This mirrors the disparity in the thermodynamic contributions to specificity seen for the four DNases binding Im proteins. We conclude that despite forming a family of structurally conserved protein complexes specificity is achieved through very different thermodynamic mechanisms, the basis of which is explored in the Discussion.

Table 3: Changes in Heat Capacity at Constant Pressure (ΔC_p) for Cognate and Representative Noncognate Complexes[a]

complex	$\Delta C_{p\ (exptl)}$ [cal/(mol K)]	$\Delta C_{p\ (calc)}$ [cal/(mol K)]	T_s[b] (K)	$\Delta S°_{HE}(T_s)$[c] [cal/(mol K)]	$\Delta S°_{rt}$[d] [cal/(mol K)]	$\Delta S°_{other}(T_s)$[e] [cal/(mol K)]
E2(+Zn^{2+})−Im2	−818	n/a	282	347	−50	−297
E2(+Zn^{2+})−Im7	−441	n/a	298	154	−50	−104
E7(+Zn^{2+})−Im7	−691	−73.73,[f] −48.33,[g] −64.65[h]	283	290	−50	−240
E7(+Zn^{2+})−Im9	−307	n/a	326	70	−50	−20
E8(+Zn^{2+})−Im7	−474	n/a	321	118	−50	−68
E8(+Zn^{2+})−Im8	−660	n/a	291	252	−50	−202
E9(+Zn^{2+})−Im2	−512	n/a	313	145	−50	−95
E9(+Zn^{2+})−Im8	−469	n/a	304	151	−50	−101
E9(+Zn^{2+})−Im9	−454	−148.59,[f] −160.74,[g] −189.71[h]	316	123	−50	−73

[a] Zn^{2+}-bound DNases were used in each case. The calculated values of ΔC_p for the E7 DNase−Im7 and E9 DNase−Im9 complexes were calculated using the equations listed below. [b] T_s is the temperature at which $\Delta S°_{total}$ (the total entropic contribution to binding) = 0 and was calculated from the entropy and heat capacity, because $\Delta C_p = d\Delta H/dT = d(T\Delta S)/dT$ and $T_s = T_o \exp(-(\Delta S(T_o)/\Delta C_p))$, where T_o = 298 K. [c] This is the calculated contribution of the hydrophobic effect to binding at T_s and assumes that the hydrophobic entropic contribution to binding is 0 at 386 K for all interactions (*74*, *75*). $\Delta S°_{HE}(T_s) = 1.35\Delta C_{p\ (exptl)} \ln(T_s/386)$ (*27*). [d] The "cratic" entropic penalty because of the restriction of rotational and translational degrees of freedom. [e] $\Delta S°_{other}(T_s) = -[\Delta S°_{HE}(T_s) + \Delta S°_{rt}]$ and is calculated on the basis of the requirement that, at T_s, $\Delta S°_{total} = 0$. [f] $(1.34\Delta ASA_{nonpolar} - 0.59\Delta ASA_{polar})/4.184$. [g] Equation 6 (see the text for details). [h] $(1.874\Delta ASA_{nonpolar} + 0.711\Delta ASA_{hydoxyl} - 1.097\Delta ASA_{polar})/4.184$ (*32*, *50*).

DISCUSSION

In the present work, we show that the thermodynamic binding parameters (ΔH, $-T\Delta S$, and ΔC_p) vary considerably between different DNase−Im protein complexes and in particular between cognate and noncognate pairings, despite the kinetic basis for specificity being conserved between DNases (*12*). Specificity is commonly viewed as a "local effect" linked to those residues that are in direct contact across the protein−ligand or protein−protein interface. However, in many interactions, mutations away from the binding site also play an important role in modulating binding affinity and specificity. In the evolution of antibody−antigen recognition, for example, somatic hypermutation and affinity maturation in antibodies can act through mutations away from the contact site, having global effects such as alteration in loop movement (*34*−*36*). We now discuss the physical basis for differences in the thermodynamics of DNase−Im protein, comparing the outcomes of this work to that on other protein−protein interactions.

Side-Chain Chemistry Partly Influences the Enthalpic and Entropic Contributions to DNase−Im Protein Binding. Polar/charged residues are thought to contribute enthalpically to binding by cooperatively forming multiple weak interactions (hydrogen bonds and salt bridges). Nonpolar residues on the other hand contribute entropically to binding (at 25 °C) as a result of the increase in disorder produced by the explusion of water that is coupled to binding (*37*−*41*). In line with this, E2 DNase−Im2, E7 DNase−Im7, and E8 DNase−Im8 cognate complexes are more polar than the E9 DNase−Im9 complex and hence more enthalpically favorable (Figures 1b and 6). Indeed, the frequency of hydrogen bonds at the E7 DNase−Im7 interface (1 per 92 Å^2) is significantly higher than at the E9 DNase−Im9 (1 per 131 Å^2) (*21*). Furthermore, the calculation of the polar and nonpolar buried surface areas from the E7 DNase−Im7 and E9 DNase−Im9 crystal structures (using Areaimol in the CCP4 suite of programs with a water probe radius of 1.4 Å) shows that, although the interfaces are of similar size (∼1600 Å^2), a more polar and less nonpolar surface area is buried at the E7 DNase−Im7 interface (−896 and −625 Å^2, respectively) compared to the E9 DNase−Im9 complex (−776 and −806 Å^2, respectively) (*7*, *21*, *22*). In the E7 DNase−Im7 complex

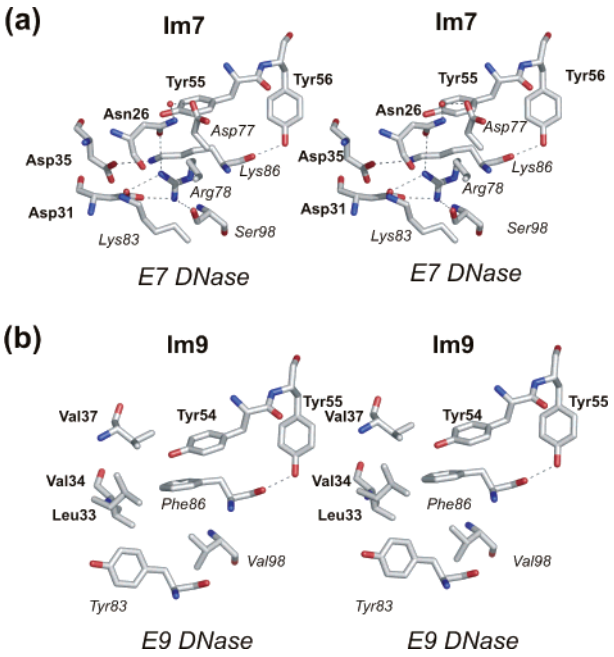

FIGURE 6: Details of the (a) E7 DNase−Im7 and (b) E9 DNase−Im9 complexes highlighting differences in specificity contacts. Im protein residues are identified in bold, and DNase residues are in italics, with the two conserved helix III tyrosine residues of each Im protein shown for orientation. The red sphere is a water that bridges an E7 DNase−Im7 specificity interaction. The PDB accessions codes for the E7 DNase−Im7 (*76*) and E9 DNase−Im9 (*21*) structures are 1mz8 and 1emv, respectively.

(Figure 6a), polar and charged specificity residues across the interface interact through hydrogen bonds and salt bridges. In the E9 DNase−Im9 complex (Figure 6b), these are replaced by nonpolar specificity residues. Thus, in principle, the change from polar to nonpolar residues could explain the observed trends in the thermodynamics noted previously.

A comparison with thermodynamic measurements on other high-affinity nuclease−inhibitor complexes is insightful. The barnase−barstar complex has a similar K_d to cognate DNase−Im protein interactions and is similarly dominated by polar and charged interactions. However, in the two published ITC studies on the interaction at pH 7.0 (*42*) and pH 8.0 (*1*), binding was found to be enthalpically driven, with either a favorable or neutral entropy. This contrasts the

significantly unfavorable entropic contributions seen for the E2 DNase−Im2, E7 DNase−Im7, and E8 DNase−Im8 complexes (Table 1), which suggests that local as well as global effects contribute to the thermodynamics of DNase−Im protein interactions. This is further addressed below in the comparative analysis of the heat capacity changes (ΔC_p) for the different complexes.

The Physical Origin of the ΔC_p of Binding Is Linked to "Global" Structural Rigidification. Rather than being static structures, biomolecules are best described as populations of conformational microstates where a molecule can take a range of accessible enthalpy levels (*H*), because of the fluctuation of structure and hydration. A rigorous statistical thermodynamic relationship (eq 4) links the changes in the range of accessible enthalpy levels that the complex occupies with the heat capacity at constant pressure (C_p), the temperature (*T*), and the Boltzmann constant (*k*) (*43*−*46*)

$$\langle H^2 \rangle - \langle H \rangle^2 = kT^2 C_p \quad (4)$$

If there is a reduction in the accessible rotational, translational, and/or vibrational energy levels coupled to binding, then the complex will have a lower heat capacity relative to the free components and a negative ΔC_p will be measured. Hence, the negative ΔC_p implies binding-induced "rigidification", namely, the reduction of thermodynamic fluctuation upon binding (*43*, *44*). As shown in eq 5, there are three possible sources that contribute to the ΔC_p, in the absence of changes in the ionization state (the case here), where simple additivity of each contribution has previously been assumed (*31*)

$$\Delta C_p = \Delta C_{p,HE} + \Delta C_{p,water} + \Delta C_{p,protein} \quad (5)$$

$\Delta C_{p,HE}$ is the contribution from the hydrophobic effect, whereby the loss of polar and nonpolar hydration is coupled to binding, $\Delta C_{p,water}$ is the contribution from trapped water molecules, and $\Delta C_{p,protein}$ is the contribution from the decrease of the degrees of rotational, translational, and vibrational freedom of the protein (which could be either or both the DNase and Im protein in the present work). In the latter case, this is often coupled to the formation of intra- and intermolecular interactions, with all types of interactions (polar and nonpolar) proposed by Cooper and co-workers to contribute to this source of ΔC_p (*28*, *40*). We discuss the relative contributions of each to the measured ΔC_p values for colicin DNase−Im protein complexes.

Changes in Polar and Nonpolar Hydration ($\Delta C_{p,HE}$) Are Comparatively Small for DNase−Im Protein Interactions. Empirical formulas, such as in eq 6, enable the $\Delta C_{p,HE}$ to be calculated from the changes in polar and nonpolar accessible surface areas (ASA) accompanying binding based on the crystal structure of the complex (*27*, *32*)

$$\Delta C_p = 0.45\Delta ASA_{nonpolar} - 0.26\Delta ASA_{polar} \quad (6)$$

Although based originally on small molecule binding and folding studies, this approach has successfully recapitulated the observed ΔC_p in some protein−protein interaction studies (*27*, *32*, *47*, *48*). The underlying assumptions of this approach are (a) that the dominant contribution to ΔC_p is $\Delta C_{p,HE}$ and thus the hydration change upon binding and (b) that this contribution is proportional to ΔASA. The physical basis for the loss of nonpolar and polar hydration having opposite effects on the calculated value of $\Delta C_{p,HE}$ is believed to be a consequence of their different hydration structures. Nonpolar hydration reduces the interaction among these waters relative to the bulk solvent, so that they have more vibrational modes accessible to them (*45*, *49*). Hence, they have a higher C_p, resulting in a decreased C_p upon the binding-induced release of nonpolar hydration. In contrast, polar hydration increases the extent of hydrogen bonding, which is relaxed upon the binding-induced release of polar hydration waters, leading to an increased C_p (*45*, *50*). The calculated $\Delta C_{p,HE}$ values are shown in Table 3 (using eq 6 and other published formulas listed in the table footnotes) for the E7 DNase−Im7 and E9 DNase−Im9 complexes and compared with their experimentally determined values. This shows that despite the E9 DNase−Im9 complex being the most nonpolar its experimentally observed ΔC_p is the least negative of all of the cognate complexes. Furthermore, for both E7 DNase−Im7 and E9 DNase−Im9, the experimentally determined ΔC_p is more negative than the calculated value; this is particularly acute for the E7 DNase−Im7 complex, where the two values differ by ∼10-fold. This observation agrees with several recent papers reporting the significant discrepancy between the prediction of ΔC_p through ΔASA-based approaches and the experimental values (*1*, *49*−*52*). This discrepancy could be due to a number of possible reasons. First, that the loss of hydration upon binding (the hydrophobic effect) does not dominate ΔC_p. This is in contrast to the approach based upon ΔASA that attributes the origin of ΔC_p directly to the hydrophobic effect. Indeed, there is a growing realization that polar groups play as important roles in defining the thermodynamics of protein−protein association, including the ΔC_p, independently from the contribution resulting from the loss of hydration coupled to binding (*28*, *40*, *41*, *53*). Second, that the contribution of the hydration change to the ΔC_p (and hence the hydrophobic effect) is not proportional to the ΔASA, which has been under debate recently (*54*−*58*). For example, Chalikian and co-workers have shown that the hydration change upon protein−protein association is far greater than the first hydration shell (the inherent assumption of the ΔASA-based approaches), instead suggesting that three hydration shells worth of waters are lost upon binding (*59*). Third, the approach based on ΔASA assumes that binding is rigid-body-like with no other processes coupled to binding. This is at odds with situations such as where point mutations are observed to have a much greater effect on ΔC_p than expected based on the loss of the buried surface area, suggesting that "nonlocal" structural changes may accompany binding and therefore impact ΔC_p (*50*, *60*−*52*). Notwithstanding these caveats, what is clear from the analysis presented here is that the ΔC_p is not predicted by surface area burial for DNase−Im protein complexes.

Differences in Observed ΔC_p Values between Cognate Complexes Are Larger Than Likely Contributions from $\Delta C_{p,water}$. We now address the role played by water molecules trapped at the DNase−Im protein interface as proposed by Ladbury and co-workers, which might explain the discrepancy between the experimental and ΔASA-based ΔC_p (*50*). Bound water molecules are frequently seen at protein−ligand interfaces by crystallography, where they increase affinity by acting as side-chain extensions, increasing complementarity and forming bridging hydrogen bonds between the

partners (*63*). Trapping of water molecules can also produce anomalously negative ΔC_p values by adding more rigidifying interactions, with a value of about −18 cal mol^{-1} K^{-1} expected per trapped water molecule (*64*). Trapping of water molecules also has an entropic penalty; Dunitz (*65*) has shown that the maximum penalty for trapping a water molecule is ∼2 kcal mol^{-1} at ∼300 K. Five and seven water molecules are trapped in the E9 DNase−Im9 and E7 DNase−Im7 complexes, respectively (*21*). While this difference could impact the observed values of ΔC_p and $-T\Delta S$, the differences between the observed values for the two complexes (Tables 1 and 3) are far larger than the contribution of two extra water molecules based on these estimates. Hence, while trapping water molecules will undoubtedly impact the thermodynamics it is unlikely to account for all of the differences between complexes.

E2, E7, and E8 DNase−Im Protein Specificity Involves Significant Protein Rigidification during Complex Formation ($\Delta C_{p,protein}$). Changes in protein dynamics can be coupled to biological specificity in protein−protein interactions. This has been demonstrated in antibody−antigen and TCR−peptide−MHC complexes, which involve flexible surface loops becoming less flexible upon ligand binding (*66*−*68*). This structural rigidification coupled to binding impacts the thermodynamics making it significantly more enthalpically favorable (because of the local folding, resulting in the gain of many favorable interactions) but more entropically unfavorable (because of the decrease in conformational freedom of the loop) than protein−protein interactions in general (*4*, *67*, *68*). Therefore, specific binding results in complex rigidification, where the ΔC_p is much more negative than expected from ΔASA-based values, illustrating how global changes are felt on the thermodynamics of binding (*4*, *67*, *68*). These effects compare well with the observed thermodynamics of cognate Im protein binding to the E2, E7, and E8 DNases, which are strongly enthalpically favorable, entropically unfavorable, and have large negative excess ΔC_p values (Tables 1 and 3).

The structural and thermodynamic analysis of ligand binding to the immunoreceptor NKG2D by McFarland and Strong is also relevant in this context (*69*). They showed that, when binding resulted in the stabilization of a loop on the ligand, ΔC_p was considerably more negative compared to another ligand where there was no loop reorganization, even when the calculated values of ΔC_p were of the same order (*69*). This is similar to the more negative ΔC_p that we observe for the cognate complexes of E2, E7, and E8 DNases relative to their noncognate counterparts (Tables 1 and 3). Spolar and Record have argued, on the basis of the thermodynamic analysis of nonspecific and specific DNA−protein complexes, that the switch from nonspecific to specific binding is accompanied by ΔC_p becoming more negative because of the reduced flexibility of protein specificity residues, which has been borne out by structural studies of *Escherichia coli lac* repressor bound to specific and nonspecific DNA (*27*, *60*).

These examples provide attractive solutions to the problem of specificity in the E2, E7, and E8 DNases, wherein specificity appears to be coupled to significant structural rigidification in cognate complexes (Table 3). However, the available crystallographic information on the free proteins and the bound complexes of the E7 DNase−Im7 complex shows no evidence of loop movements or indeed of any other large-scale conformational changes (*17*, *20*, *22*), a feature shared with the E9 DNase−Im9 complex (*18*, *19*, *21*, *26*). Instead, the structural rigidification coupled to specificity more likely takes the form of a reduction in the conformational dynamics of the native state ensemble of one or both of the proteins that is not observed by crystallography. This rigidification is distinct from that accompanying Zn^{2+} binding the DNase (*18*, *19*, *21*, *26*) because the relative differences in the ΔH between the metal-free and Zn^{2+}-bound DNases shown in Table 1 for cognate binding also occur upon noncognate binding (data not shown). Nevertheless, a "global" response upon cognate formation implies that alteration of residues away from the interface could affect affinity. Such "framework" effects are a notable feature of the evolution of high affinity by somatic hypermutation in antibody interactions (*35*, *36*), which as mentioned above share similar binding thermodynamics. When Bernath et al. used in vitro compartmentalization to evolve Im9 to bind tighter to the E7 DNase, the cognate-binding affinity was not achieved, despite the presence of the same specificity residues as seen in the E7 DNase−Im7 structure (Figure 6) (*71*). Thus, the structural framework upon which the residues are presented could be important, such that only when this is correct can cognate DNase−Im protein binding be achieved and the observed reduction in conformational dynamics be produced. We note that an alternative explanation exists in which individual residues at an interface can have a greater than expected impact on the observed ΔC_p as previously observed for a number of systems (*50*, *60*, *61*). Such a residue mediates a network of cooperative hydrogen-bonding interactions in the case of TATA-binding protein−DNA binding (*50*), with a hydrogen-bond network mediating specificity at the E7 DNase−Im7 interface (Figure 6).

Protein Structural Rigidification Is Not Coupled to E9 DNase−Im Protein Specificity. The specificity of cognate Im protein binding for the E2, E7, and E8 DNases is coupled to binding, becoming entropically unfavorable and ΔC_p more negative relative to noncognate complexes. This "thermodynamic signature" for specificity is however different for the E9 DNase, where the cognate complex is entropically more favorable than noncognate complexes, with both types of complexes having similar ΔC_p values. This suggests that despite the high sequence identity among the four DNase domains and Im proteins, structural changes are not coupled to specificity for the E9 DNase. This is consistent with our recent kinetic analysis of E9 DNase−Im protein binding, which suggested that conformational changes accompanying binding likely take the form of rigid-body rotations, rather than induced-fit or pre-equilibrium conformational changes, as seen in TCR−peptide−MHC and antibody−antigen complexes, respectively (*66*, *68*). Hence, specificity at the E9 DNase instead has a different thermodynamic basis, which we address below.

In the case of high-affinity Kazal inhibitors of serine proteases, binding is entropically driven through the loss of hydration upon binding, with binding being essentially rigid-body (*59*, *72*). Hence, the origin of the more entropically favorable binding of the cognate E9 DNase−Im9 complex could be coupled to specificity-linked exclusion of hydrophobic hydration. This assertion is supported by the fact that the two Im9 helix II residues, which protein engineering has

shown to be involved in specificity (Leu33 and Val34), are nonpolar. Furthermore, the E9 DNase−Im9 crystal structure (Figure 6) shows that Im9 Leu33 and Val34 form a hydrophobic patch at the interface along with the alkyl chains of nonpolar E9 DNase residues, which have also been implicated in specificity (*73*). Hence, specificity residues on the E9 DNase and Im9 form complementary protein surfaces, with little room for explicit water. To further test this idea, we measured the thermodynamics of E9 DNase binding to the Im9 L33A mutant (which kinetic experiments have previously shown to destabilize binding by 3.4 kcal mol^{-1}) (*15*). Values for ΔH and $-T\Delta S$ of −9.71 (±0.08) and −5.44 kcal mol^{-1}, respectively, were measured. A comparison with the wild-type complex (Table 1) shows that the destabilizing effect of the mutation arises from the entropic [$\Delta(-T\Delta S) =$ 2.63 kcal mol^{-1}] rather than enthalpic ($\Delta\Delta H = 0.8$ kcal mol^{-1}) contribution, consistent with the Im9 Leu33 stabilizing binding by exclusion of hydrophobic hydration. Thus, the hydrophobic effect is important for specificity in the E9 DNase−Im9 complex. In comparison, the mutation of a conserved helix III hotspot residue (Im9 Tyr55) weakens cognate binding solely through the loss of favorable enthalpy {$\Delta\Delta G = 4.6$ kcal mol^{-1} (*15*), $\Delta H = -5.0$ (±0.12) kcal mol^{-1} ($\Delta\Delta H = 5.5$ kcal mol^{-1}), and $-T\Delta S = -9.17$ kcal mol^{-1} [$\Delta(-T\Delta S] = -1$ kcal mol^{-1})}, with this mutation having similar effects in noncognate complexes (data not shown). Importantly, whereas the two key helix II specificity residues on Im9 are nonpolar (Leu33 and Val34), the equivalent residues on Im2 are charged and polar residues (Asp33 and Asn34). This would preclude the expulsion of interfacial water and the formation of a complementary protein interface, explaining the less entropically favored binding of the E9 DNase by Im2 and slightly more negative ΔC_p.

In general, the residues at the specificity sites for the cognate complexes of the E2, E7, and E8 DNases are polar and/or charged, while these are nonpolar for the E9 DNase. Importantly, if all DNase−Im protein complexes were to use nonpolar residues at such sites, the observed high level of specificity (cognate binding 10^6−10^{10} tighter than noncognate) (*10*, *11*) would not be possible. Hence, evolution has selected a variety of polar and charged and nonpolar amino acids as DNase−Im protein specificity residues, thereby maintaining high levels of discrimination between complexes, with the consequence being different thermodynamic mechanisms underpin specificity for different complexes.

In conclusion, we have characterized the thermodynamics (ΔH, $-T\Delta S$, and ΔC_p) of colicin DNase−Im protein binding to probe the thermodynamic basis of specificity. This has shown that, despite noncognate complexes binding over a narrow range of affinities, this is achieved by widely differing enthalpic and entropic contributions to binding. Such "enthalpy−entropy" compensation likely reflects the diversity of interactions that are made at the different complexes. Importantly, we show that specificity in colicin DNase−Im protein complexes is underpinned by two distinct thermodynamic signatures even though they share the same kinetic signatures for specificity. For the E2, E7, and E8 DNases, the present work indicates that specificity is coupled to conformational changes most likely taking the form of side-chain rigidification in the context of cognate complexes. A detailed investigation of the change in side-chain dynamics by NMR upon binding would illuminate this speculation further. In contrast, such changes appear not to play a significant role in E9 DNase specificity, which is instead coupled to the exclusion of surface waters in the context of the cognate complex. What is perhaps most striking is the fact that despite all of these differences in the observed thermodynamics, binding results in the burial of a conserved epitope (helix III on the Im proteins) in all cases and involves a conserved binding mechanism that involves essentially "rigid-body rotations" after the formation of the initial encounter complex allowing for optimal alignment of specificity residues (*16*). The differences in the thermodynamics of specificity thus reflect the presence of two strikingly different events coupled to these rotations: the formation of hydrogen-bonding networks by the E2, E7, and E8 DNase and the exclusion of water from hydrophobic surfaces for the E9 DNase.

ACKNOWLEDGMENT

We thank Andrew Leech for expert technical advice and Maria-Jesus Mate for assistance with the Areaimol calculations.

REFERENCES

1. Frisch, C., Schreiber, G., Johnson, C. M., and Fersht, A. R. (1997) Thermodynamics of the interaction of barnase and barstar: Changes in free energy versus changes in enthalpy on mutation, *J. Mol. Biol. 267*, 696−706.
2. Willcox, B. E., Gao, G. F., Wyer, J. R., Ladbury, J. E., Bell, J. I., Jakodsen, B. K., and van der Merwe, P. A. (1999) TCR binding to peptide−MHC stabilizes a flexible recognition interface, *Immunity 10*, 357−365.
3. Kiel, C., Serrano, L., and Herrmann, C. (2004) A detailed thermodynamic analysis of ras/effector complex interfaces, *J. Mol. Biol. 340*, 1039−1058.
4. Stites, W. E. (1997) Protein−protein interactions: Interface structure, binding thermodynamics, and mutational analysis, *Chem. Rev. 97*, 1233−1250.
5. Pommer, A. J., Cal, S., Keeble, A. H., Walker, D., Evans, S. J., Kühlmann, U. C., Cooper, A., Connolly, B. A., Hemmings, A. M., Moore, G. R., James, R., and Kleanthous, C. (2001)-Mechanism and cleavage specificity of the H−N−H endonuclease colicin E9, *J. Mol. Biol. 314*, 735−749.
6. Kleanthous, C., Hemmings, A. M., Moore, G. R., and James, R. (1998) Immunity proteins and their specificity for endonuclease colicins: Telling right from wrong in protein−protein recognition, *Mol. Microbiol. 28*, 227−233.
7. Kleanthous, C., Kühlmann, U. C., Pommer, A. J., Ferguson, N., Radford, S. E., Moore, G. R., James, R., and Hemmings, A. M. (1999) Structural and mechanistic basis of immunity toward endonuclease colicins, *Nat. Struct. Biol. 6*, 243−252.
8. Pommer, A. J., and Kleanthous, C. (2000) Nuclease inhibitors, in *Frontiers in Molecular Biology: Protein−Protein Recognition* (Kleanthous, C., Ed.) Oxford University Press, Oxford, U.K.
9. Kleanthous, C., and Walker, D. (2001) Immunity proteins: Enzyme inhibitors that avoid the active site, *Trends Biochem. Sci. 26*, 624−631.
10. Wallis, R., Moore, G. R., James, R., and Kleanthous, C. (1995) Protein−protein interactions in colicin E9 DNase−immunity protein complexes. 1. Diffusion-controlled association and femtomolar binding for the cognate complex, *Biochemistry 34*, 13743−13750.
11. Wallis, R., Leung, K.-Y., Pommer, A. J., Videler, H., Moore, G. R., James, R., and Kleanthous, C. (1995) Protein−protein interactions in colicin E9 DNase−immunity protein complexes. 2. Cognate and non-cognate interactions that span the millimolar to femtomolar affinity range, *Biochemistry 34*, 13751−13759.
12. Li, W., Keeble, A. H., Giffard, C., James, R., Moore, G. R., and Kleanthous, C. (2004) Highly discriminating protein−protein interaction specificities in the context of a conserved binding energy hotspot. *J. Mol. Biol. 337*, 743−759.

13. Li, W., Dennis, C. A., Moore, G. R., James, R., and Kleanthous, C. (1997) Protein−protein interaction specificity of Im9 for the endonuclease toxin colicin E9 defined by homologue-scanning mutagenesis, *J. Biol. Chem. 272*, 22253−22258.
14. Li, W., Hamill, S. J., Hemmings, A. M., Moore, G. R., James, R., and Kleanthous, C. (1998) Dual recognition and the role of specificity-determining residues in colicin E9 DNase−immunity protein interactions, *Biochemistry 37*, 11771−11779.
15. Wallis, R., Leung, K.-Y., Osborne, M. J., James, R., Moore, G. R., and Kleanthous, C. (1998) Specificity in protein−protein recognition: Conserved Im9 residues are the major determinants of stability in the colicin E9 DNase−Im9 complex, *Biochemistry 37*, 476−485.
16. Keeble, A. H., and Kleanthous, C. (2005) The kinetic basis for dual recognition in colicin endonuclease−immunity protein complexes, *J. Mol. Biol. 352*, 656−671.
17. Dennis, C. A., Videler, H., Pauptit, R. A., Wallis, R., James, R., Moore, G. R., and Kleanthous, C. (1998) A structural comparison of the colicin immunity proteins Im7 and Im9 gives new insights into the molecular determinants of immunity-protein specificity, *Biochem. J. 333*, 183−191.
18. Kolade, O. O., Carr, S. B., Kühlmann, U. C., Pommer, A., Kleanthous, C., Bouchcinsky, C. A., and Hemmings, A. M. (2002) Structural aspects of the inhibition of DNase and rRNase colicins by their immunity proteins, *Biochimie 84*, 439−446.
19. Whittaker, S. B., Czisch, M., Wechselberger, R., Kaptein, R., Hemmings, A. M., James, R., Kleanthous, C., and Moore, G. R. (2000) Slow conformational dynamics of an endonuclease persist in its complex with its natural protein inhibitor, *Protein Sci. 9*, 713−720.
20. Cheng, Y. S., Hsia, K. C., Doudeva, L. G., Chak, K. F., and Yuan, H. S. (2002) The crystal structure of the nuclease domain of colicin E7 suggests a mechanism for binding to double-stranded DNA by the H−N−H endonucleases, *J. Mol. Biol. 324*, 227−236.
21. Kühlmann, U. C., Pommer, A. J., Moore, G. R., James, R., and Kleanthous, C. (2000) Specificity in protein−protein interactions: The structural basis for dual recognition in endonuclease colicin−immunity protein complexes, *J. Mol. Biol. 301*, 1163−1178.
22. Ko, T. P., Liao, C. C., Ku, W. Y., Chak, K. F., and Yuan, H. S. (1999) The crystal structure of the DNase domain of colicin E7 in complex with its inhibitor Im7 protein, *Structure 7*, 97−102.
23. Cooper, A. (1996) Thermodynamic analysis of biomolecular interactions, *Curr. Opin. Chem. Biol. 3*, 557−563.
24. Keeble, A. H., Hemmings, A. M., James, R., Moore, G. R., and Kleanthous, C. (2002) Multistep binding of transition metals to the H−N−H endonuclease toxin colicin E9, *Biochemistry 41*, 10234−10244.
25. Pommer, A. J., Kühlmann, U. C., Cooper, A., Hemmings, A. M., Moore, G. R., James, R., and Kleanthous, C. (1999) Homing in on the role of transition metals in the HNH motif of colicin endonucleases, *J. Biol. Chem. 274*, 27153−27160.
26. van den Bremer, E. T., Keeble, A. H., Jiskoot, W., Spelbrink, R. E., Maier, C. S., van Hoek, A., Visser, A. J., James, R., Moore, G. R., Kleanthous, C., and Heck, A. J. (2004) Distinct conformational stability and functional activity of four highly homologous endonuclease colicins, *Protein Sci. 13*, 1391−1401.
27. Spolar, R. S., and Record, M. T., Jr. (1994) Coupling of local folding to site-specific binding of proteins to DNA, *Science 263*, 777−784.
28. Cooper, A., Johnson, C. M., Lakey, J. H., and Nollmann, M. (2001) Heat does not come in different colours: Entropy−enthalpy compensation, free energy windows, quantum confinement, pressure perturbation calorimetry, solvation and the multiple causes of heat capacity effects in biomolecular interactions, *Biophys. Chem. 93*, 215−230.
29. Baker, B. M., and Murphy, K. P. (1996) Evaluation of linked protonation effects in protein binding reactions using isothermal titration calorimetry, *Biophys. J. 71*, 2049−2055.
30. Fukada, H., and Takahashi, K. (1998) Enthalpy and heat capacity changes for the proton dissociation of various buffer components in 0.1 M potassium chloride, *Proteins: Struct., Funct., Genet. 33*, 159−166.
31. Dunitz, J. D. (1995) Win some, lose some: Enthalpy−entropy compensation in weak intermolecular interactions, *Chem. Biol. 2*, 709−712.
32. Gomez, J., and Freire, E. (1995) Thermodynamic mapping of the inhibitor site of the aspartic protease endothiapepsin, *J. Mol. Biol. 252*, 337−350.
33. Hannan, J. P., Whittaker, S. B., Hemmings, A. M., James, R., Kleanthous, C., and Moore, G. R. (2000) NMR studies of metal ion binding to the Zn-finger-like HNH motif of colicin E9, *J. Inorg. Biochem. 79*, 365−370.
34. Foote, J., and Milstein, C. (1991) Kinetic maturation of an immune response, *Nature 352*, 530−532.
35. Foote, J., and Winter, G. (1992) Antibody framework residues affecting the conformation of the hypervariable loops, *J. Mol. Biol. 224*, 487−499.
36. Hawkins, R. E., Russell, S. J., Baier, M., and Winter, G. (1993) The contribution of contact and non-contact residues of antibody in the affinity of binding to antigen. The interaction of mutant D1.3 antibodies with lysozyme, *J. Mol. Biol. 234*, 958−964.
37. Kauzmann, W. (1959) Some factors in the interpretation of protein denaturation, *Adv. Protein Chem. 14*, 1−63.
38. Privalov, P. L., and Gill, S. J. (1988) Stability of protein structure and hydrophobic interaction, *Adv. Protein Chem. 39*, 191−234.
39. Dill, K. A. (1990) Dominant forces in protein folding, *Biochemistry 29*, 7133−7155.
40. Cooper, A. (2000) Heat capacity of hydrogen-bonded networks: An alternative view of protein folding thermodynamics, *Biophys. Chem. 85*, 25−39.
41. Pace, C. N. (2001) Polar group burial contributes more to protein stability than nonpolar group burial, *Biochemistry 40*, 310−313.
42. Martinez, J. C., Filimonov, V. V., Mateo, P. L., Schreiber, G., and Fersht. AR. (1995) A calorimetric study of the thermal stability of barstar and its interaction with barnase, *Biochemistry 34*, 5224−5233.
43. Cooper, A. (1976) Thermodynamic fluctuations in protein molecules, *Proc. Natl. Acad. Sci. U.S.A. 73*, 2740−2741.
44. Cooper, A. (1984) Protein fluctuations and the thermodynamic uncertainty principle, *Prog. Biophys. Mol. Biol. 44*, 181−214.
45. Sturtevant, J. M. (1977) Heat capacity and entropy changes in processes involving proteins, *Proc. Natl. Acad. Sci. U.S.A. 74*, 2236−2240.
46. Eftink, M. R, Anusiem, A. C., and Biltonen, R. L. (1983) Enthalpy−entropy compensation and heat capacity changes for protein−ligand interactions: General thermodynamic models and data for the binding of nucleotides to ribonuclease A, *Biochemistry 22*, 3884−3896.
47. Spolar, R. S., Livingstone, J. R., and Record, M. T., Jr. (1992) Use of liquid hydrocarbon and amide transfer data to estimate contributions to thermodynamic functions of protein folding from the removal of nonpolar and polar surface from water, *Biochemistry 31*, 3947−3955.
48. Baker, B. M., and Murphy, K. P. (1997) Dissecting the energetics of a protein−protein interaction: The binding of ovomucoid third domain to elastase, *J. Mol. Biol. 268*, 557−569.
49. Scatena, L. F., Brown, M. G., and Richmond, G. L. (2001) Water at hydrophobic surfaces: Weak hydrogen bonding and strong orientation effects, *Science 292*, 908−912.
50. Bergqvist, S., Williams, M. A., O'Brien, R., and Ladbury, J. E. (2004) Heat capacity effects of water molecules and ions at a protein−DNA interface, *J. Mol. Biol. 336*, 829−842.
51. Loladze, V. V., Ermolenko, D. N., and Makhatadze, G. I. (2001) Heat capacity changes upon burial of polar and nonpolar groups in proteins, *Protein Sci. 10*, 1343−1352.
52. Henriques, D. A., Ladbury, J. E., and Jackson, R. M. (2000) Comparison of binding energies of SrcSH2-phosphotyrosyl peptides with structure-based prediction using surface area based empirical parameterization, *Protein Sci. 9*, 1975−1985.
53. Ross, P. D., and Subramanian, S. (1981) Thermodynamics of protein association reactions: Forces contributing to stability, *Biochemistry 20*, 3096−3102.
54. Shimizu, S., and Chan, H. S. (2001) Configuration-dependent heat capacity of pairwise hydrophobic interactions, *J. Am. Chem. Soc. 123*, 2083−2084.
55. Shimizu, S., and Chan, H. S. (2002) Origins of protein denatured state compactness and hydrophobic clustering in aqueous urea: Inferences from nonpolar potentials of mean force, *Proteins 49*, 560−566.
56. Rick, S. W. (2003) Heat capacity change of the hydrophobic interaction, *J. Phys. Chem. B 197*, 9853−9857.
57. Paschek, D. (2004) Temperature dependence of the hydrophobic hydration and interaction of simple solutes: An examination of five popular water models, *J. Chem. Phys. 120*, 6674−6690.
58. Paschek, D. (2004) Heat capacity effects associated with the hydrophobic hydration and interaction of simple solutes: A

detailed structural and energetical analysis based on molecular dynamics simulations, *J. Chem. Phys. 120*, 10605−10617.
59. Filfil, R., and Chalikian, T. V. (2003) The thermodynamics of protein−protein recognition as characterized by a combination of volumetric and calorimetric techniques: The binding of turkey ovomucoid third domain to α-chymotrypsin, *J. Mol. Biol. 326*, 1271−1288.
60. Jung, H. I., Cooper, A., and Perham, R. N. (2002) Identification of key amino acid residues in the assembly of enzymes into the pyruvate dehydrogenase complex of *Bacillus stearothermophilus*: A kinetic and thermodynamic analysis, *Biochemistry 41*, 10446−10453.
61. Wibbenmeyer, J. A., Schuck, P., Smith-Gill, S. J., and Willson, R. C. (1999) Salt links dominate affinity of antibody HyHEL-5 for lysozyme through enthalpic contributions, *J. Biol. Chem. 274*, 26838−26842.
62. Ladbury, J. E., and Williams, M. A. (2004) The extended interface: Measuring non-local effects in biomolecular interactions, *Curr. Opin. Struct. Biol. 14*, 562−569.
63. Janin, J. (1999) Wet and dry interfaces: The role of solvent in protein−protein and protein−DNA recognition, *Struct. Fold Des. 7*, R277−R279.
64. Cooper, A. (2005) Heat capacity effects in protein folding and ligand binding: A re-evaluation of the role of water in biomolecular thermodynamics, *Biophys Chem. 115*, 89−97.
65. Dunitz, J. D. (1994) The entropic cost of bound water in crystals and biomolecules, *Science 264*, 670.
66. James, L. C., Roversi, P., and Tawfik, D. S. (2003) Antibody multispecificity mediated by conformational diversity, *Science 299*, 1362−1367.
67. Willcox, B. E., Gao, G. F., Wyer, J. R., Ladbury, J. E., Bell, J. I., Jakobsen, B. K., and van der Merwe, P. A. (1999) TCR binding to peptide−MHC stabilizes a flexible recognition interface, *Immunity 10*, 357−365.
68. Krogsgaard, M., Prado, N., Adams, E. J., He, X. L., Chow, D. C., Wilson, D. B, Garcia, K. C., and Davis, M. M. (2003) Evidence that structural rearrangements and/or flexibility during TCR binding can contribute to T cell activation, *Mol. Cell 12*, 1367−1378.
69. McFarland, B. J., and Strong, R. K. (2003) Thermodynamic analysis of degenerate recognition by the NKG2D immunoreceptor: Not induced fit but rigid adaptation, *Immunity 19*, 803−812.
70. Kalodimos, C. G., Biris, N., Bonvin, A. M., Levandoski, M. M., Guennuegues, M., Boelens, R., and Kaptein, R. (2004) Structure and flexibility adaptation in nonspecific and specific protein−DNA complexes, *Science 305*, 386−389.
71. Bernath, K., Magdassi, S., and Tawfik, D. S. (2005) Directed evolution of protein inhibitors of DNA−nucleases by in vitro compartmentalization (IVC) and nano-droplet delivery, *J. Mol. Biol. 345*, 1015−1026.
72. Horn, J. R., Ramaswamy, S., and Murphy, K. P. (2003) Structure and energetics of protein−protein interactions: The role of conformational heterogeneity in OMTKY3 binding to serine proteases, *J. Mol. Biol. 331*, 497−508.
73. Curtis, M. D., and James, R. (1991) Investigation of the specificity of the interaction between colicin E9 and its immunity protein by site-directed mutagenesis, *Mol Microbiol. 5*, 2727−2733.
74. Baldwin, R. L. (1986) Temperature dependence of the hydrophobic interaction in protein folding, *Proc. Natl. Acad. Sci. U.S.A.* 83, 8069−8072.
75. Murphy, K. P., Privalov, P. L., and Gill, S. J. (1990) Common features of protein unfolding and dissolution of hydrophobic compounds, *Science 247*, 559−561.
76. Sui, M. J., Tsai, L. C., Hsia, K, C., Doudeva, L. G., Ku, W. Y., Han, G. W., and Yuan, H. S. (2002) Metal ions and phosphate binding in the H−N−H motif: Crystal structures of the nuclease domain of ColE7/Im7 in complex with a phosphate ion and different divalent metal ions, *Protein Sci. 11*, 2947−2957.

BI052373O